17. Microfluidic Micro/Nano Droplets

Gopakumar Kamalakshakurup, Derek Vallejo, Abraham Lee

Microfluidic droplet technology has evolved rapidly since the first microfluidic droplet generator was reported over a decade ago. It has subsequently branched out and emerged as a practical solution to enhance the capabilities of many other fields, including, but not limited to: high-throughput screening, biosensing, drug delivery and synthetic biology. In this chapter, we will report on recent advancements in droplet microfluidic technologies that have emerged since *Teh* et al.'s comprehensive 2007 review. We begin with a brief history of droplet microfluidics and introduce methods of droplet production, manipulation, and sensing methodologies. The remainder of the chapter is dedicated to design considerations for various droplet production configurations, concluding with a discussion on applications, trends and the general direction that the field is headed.

17.1 Introduction to Micro/Nano Droplet Microfluidic Technologies

High-throughput screening (HTS) is a scientific method to conduct millions of chemical and biological reactions. A typical example of HTS is the discovery of drugs in the pharmaceutical industry, where millions of drug compounds are tested against the target samples to analyze the activity. Since early 1960s, screening has been performed using microplate technology and it is still a convenient platform used by many HTS industries. If we take an example of drug screening in pharmaceutical industry, the process flow occurs in three steps as shown in Fig. 17.1:

1. Biological target samples are pipetted into the well plates
2. Drug compounds are added to the wells
3. The fluorescent activity is captured using a detector that scans the wells.

The limitations of this technology includes:

1. Reagent and sample consumption. Each well consumes milliliter volumes of reagents, which increases the cost of screening. To reduce the reagent consumption, attempts have made to incorporate a higher number of miniaturized wells (Moore's law of miniaturization). In general, 96 well plates are considered standard, but companies like DuPont have come up with 9600 well plates. This leads to another limitation of liquid handling.
2. Using 96 well plates, one can use pipettes to manually load the samples, but 9600 well plates require robotic pipetting, which again increases the cost of screening.
3. Evaporation and contamination. Reagents/samples can evaporate from the wells and can also cause contamination issues.
4. Low throughput. To perform millions of reactions, the microplate platform takes several days. These limitations forced the scientific community to come up with an alternate solution to microplate technology.

Advancements in microfabrication technology revolutionized the process of sensing and detection of chemical and biological samples [17.1]. The samples
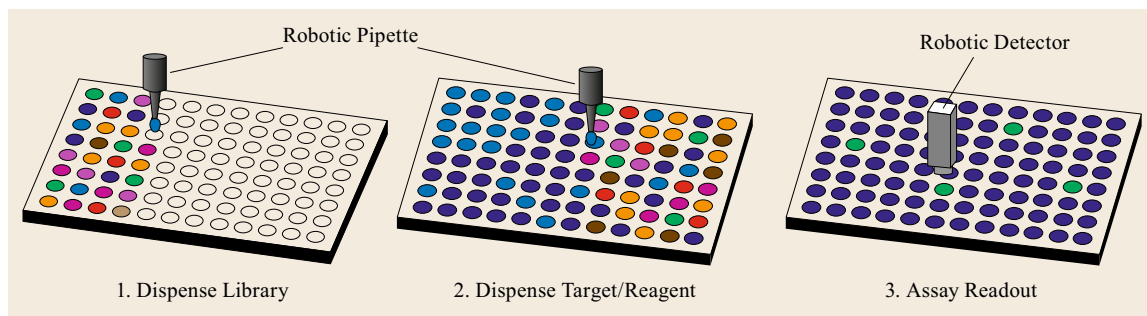
Fig. 17.1 Drug screening process in microplate format: 1. Biological sample is pipetted into the wells 2. The reagent or drug compound is dispensed into the wells. 3. The aftereffect of the reaction is detected using a robotic scanner

are manipulated and analyzed in miniaturized microfluidic chips often referred to as *lab on chip* devices. Depending on the liquid manipulation methodology, we can classify microfluidics into two groups: single-phase (or continuous) microfluidics and multiphase (or droplet) microfluidics. Single-phase microfluidics deals with manipulation of miscible liquids inside a microfluidic chip. Using single-phase technology, numerous chemical or biological reactions can be performed by integrating thousands of micromechanical valves and control components [17.2] (Fig. 17.2). These systems are referred to as microfluidic large scale integration [17.3]. However, single-phase microfluidics has limitations:

1. Samples directly interact with the channel walls and cause cross-contamination of fluid constituents
2. Scaling-up of the screening process require additional chambers and valves, leading to an increase in overall chip size
3. Reagent consumption, though microliters (μL) in volume, could become significant in large-scale screening.

Attempts to overcome the limitations of single-phase microfluidics led to the evolution of the second category of microfluidics referred to as multiphase microfluidics. The most popular form of multiphase microfluidics is droplet microfluidics. Droplet microfluidics deals with the manipulation of nanoliter (nl) to femtoliter (fl) droplets inside microfluidic channels [17.4]. Each droplet can act as an isolated reaction container for biochemical assays while offering several advantages over conventional single-phase methods:

1. Droplets can have volumes as little as femtoliters, leading to a reduction in reagent consumption and therefore the cost of biological screening.

2. The thin layer of carrier phase around the droplet prevents evaporation or contamination; droplets can be generated and detected with ultrafast assay throughputs (rates up to 10 KHz).
3. In droplet format, we can perform millions of chemical or biological reactions in minutes. One of the most important advantages is that droplet microfluidic technology can perform operations that can emulate laboratory benchtop processes, such as fluid dispensing, mixing, aliquot and sorting/separation.
4. Fluid dispensing is analogous to droplet generation; mixing, aliquot and separation is equivalent to droplet merging, droplet splitting and droplet sorting, respectively.

These unit operations make the droplet technology feasible for HTS of chemical or biological assays. Here we describe and discuss the droplet unit operations in detail.

17.1.1 Droplet Generation

One critical aspect of droplet microfluidics is the ability to generate stable, uniformly sized droplets. Precise control over the parameters, including channel geometry, the flowrate of two phases (shear force), the viscosity of the phases and the interfacial tension between the phases, are critical to achieve reliable droplet production. The two basic (and most commonly adopted) device configurations to generate droplets are T-junction and flow-focusing geometries.

T–Junction Configuration
In this configuration, the dispersed phase and the continuous stream intersect perpendicular to each other [17.5]. The continuous phase exerts unidirectional shear on the dispersed phase (Fig. 17.3). As the dispersed phase gradually fills the main channel, it im-
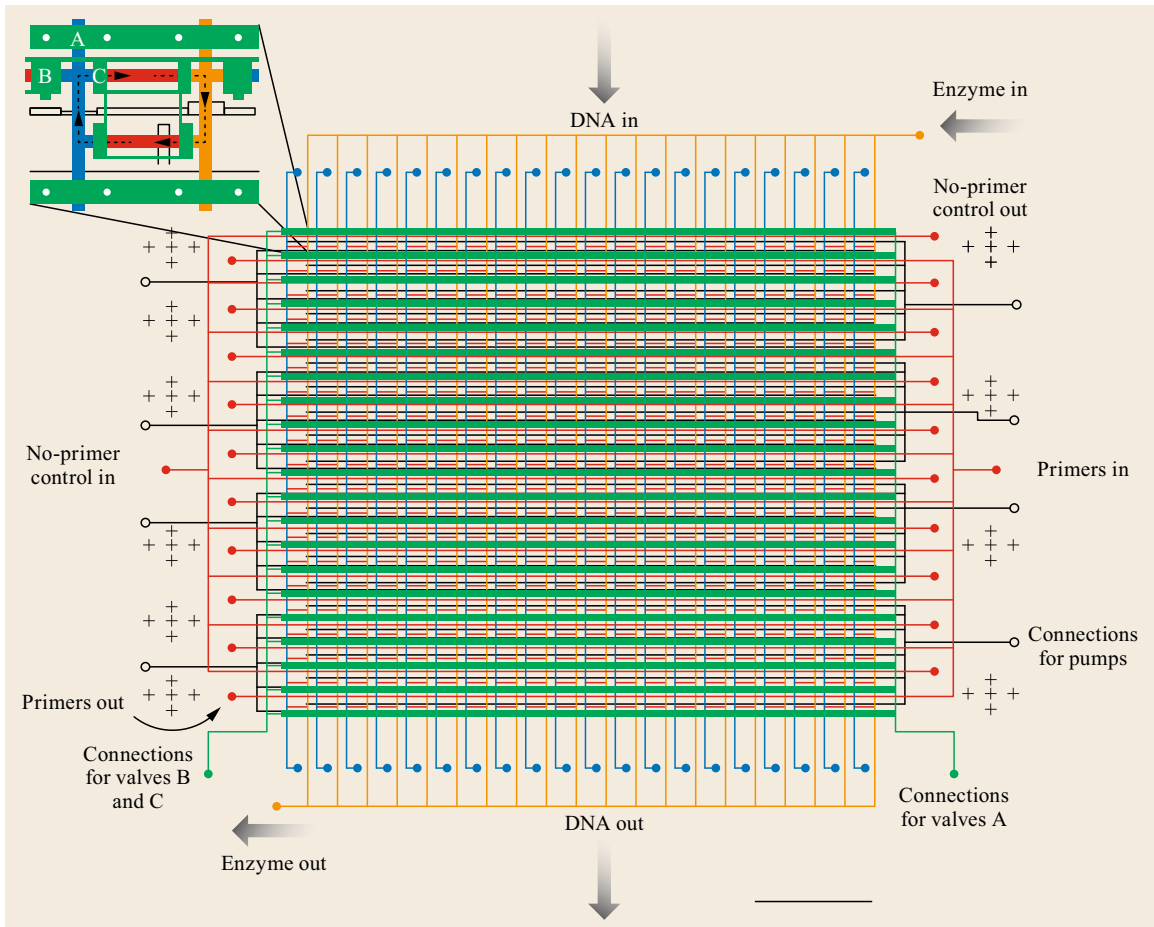
Fig. 17.2 Schematic of a microfluidic large-scale integration device. It consists of 25×40 chambers and each chamber can hold 250 picoliters of sample volume (after [17.3])
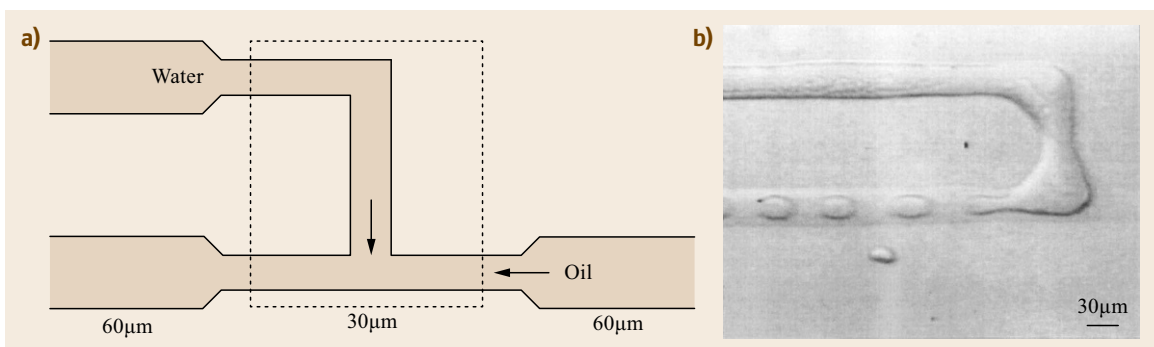

Fig. 17.3 (a) Schematic of first T-junction geometry reported in 2001. T-junction microfluidic droplet generator. **(b)** Reprinted with permission from [17.5], copyright 2001 by the American Physical Society

pedes the continuous phase flow, resulting in a pressure buildup in the main channel and leading to the droplet pinch-off. To perform more sophisticated assays, alternate droplet generators are implemented with multiple T-junctions enabling simultaneous introduction of multiple reagents and sample solutions (Fig. 17.4) [17.6].
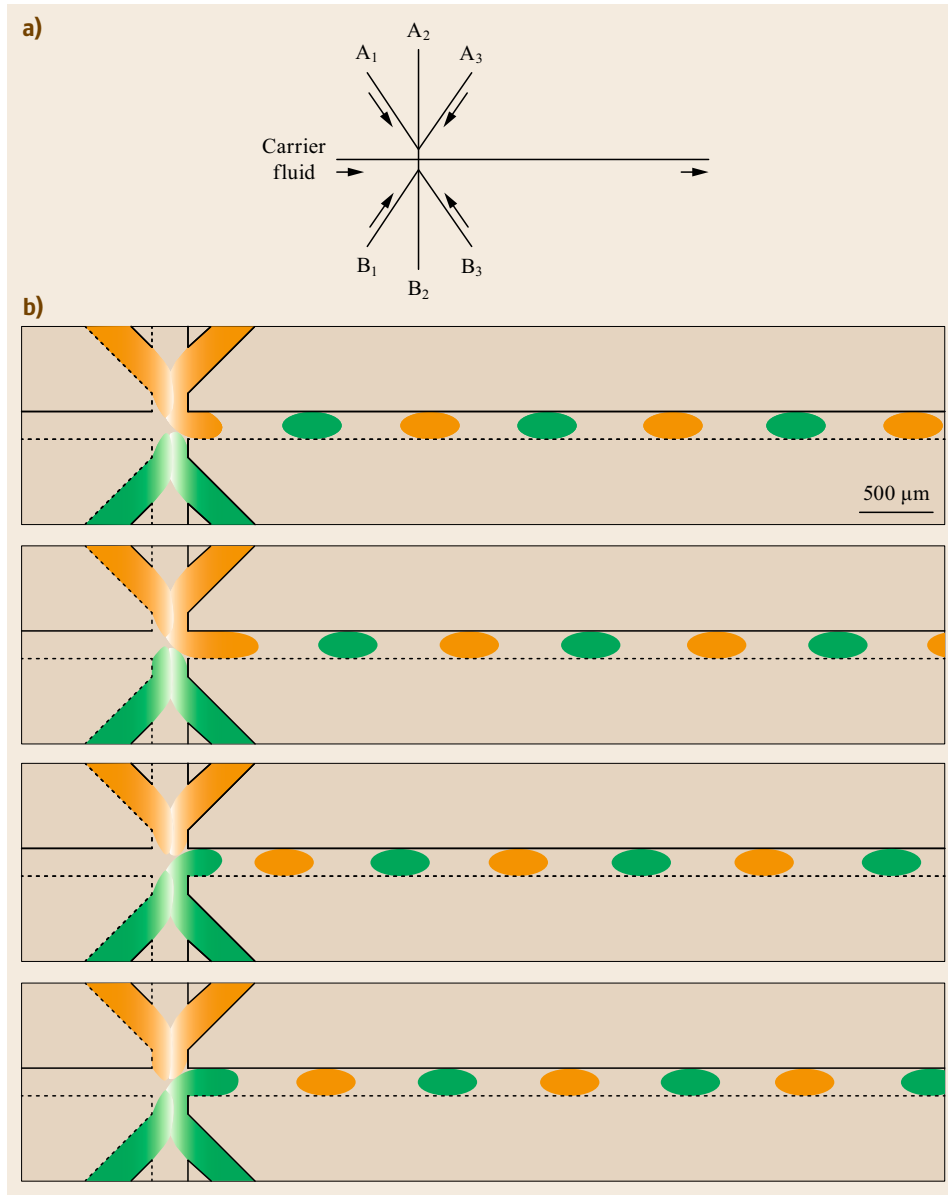
Fig. 17.4a,b Alternating T-junction droplet generator. (a) Schematic of the microfluidic chip (b) Sequential images illustrating the detailed process of alternate droplet generation

Flow–Focusing Configuration

In this configuration, both the dispersed and continuous phases are forced to pass through a narrow orifice in the microfluidic device in a sheath flow fashion (dispersed phase sandwiched by two continuous phase streams) (Fig. 17.5 and 17.6) [17.7]. The flow-focusing droplet generation can be explained by a simplified model. When the dispersed phase enters the junction, it blocks the flow of continuous phase resulting in a pressure buildup in the continuous phase inlets. The subsequent shear, as a result of the pressure buildup, pinches off the dispersed phase to form droplets. This process of droplet breakup is valid only for geometry-controlled regime, and not applicable for all droplet generation regimes. The physical principles of droplet generation and techniques are described in Sect. 17.3. Recently, it was reported that $10-50\,\mathrm{fl}$ droplets can be generated at frequencies ranging from 200 to 1.3 MHz, enabling droplet technology as an ultrahigh-throughput screening platform [17.8]. Parallel droplet generation is an alternative method to increase the throughput by interconnecting networks of individual droplet generators. This can achieve ultrahigh throughput albeit the complexity of the system increases with multiplexing.
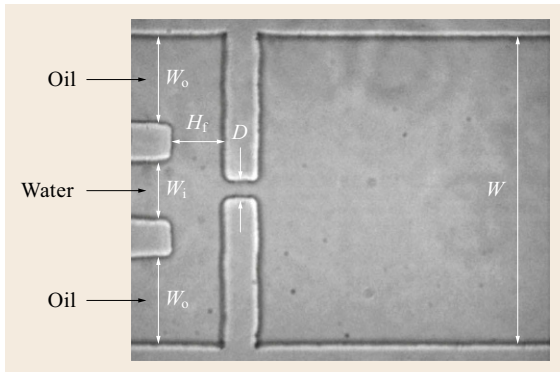
Fig. 17.5 Microfluidic flow-focusing droplet generator device. Reprinted from [17.7] with the permission of AIP Publishing

An example of parallelization is a three-dimensional monolithic elastomer device with an array of 20×50 flow-focusing generators capable of generating droplets at 8.7 MHz, the highest droplet generation rate reported to date (Fig. 17.7) [17.9]. In most cases, the microfluidic devices are manufactured using polydimethyl siloxane (PDMS), which is an inexpensive, flexible and transparent elastomeric polymer [17.10].

17.1.2 Droplet Merging

Automated droplet fusion is also a critical unit operation, where the independently generated droplets of reagents and samples are subjected to controlled merging and the activity of the merged droplets is monitored using droplet detection technologies.

Passive Merging
Passive techniques utilize microfluidic channel designs to ensure controlled merging. There are several ways to perform passive droplet fusion. However, the two eminent techniques are based on channel expansion [17.11]

and pillar designs [17.12]. When a droplet encounters a channel expansion, the decrease in velocity slows down the droplet ensuring merging with the preceding droplet (Fig. 17.8). In the pillar-induced technique, the continuous phase near the droplet drains through the gap between the pillars. This slows down the droplet and eventually enables merging with the successive droplets until the hydrostatic pressure exceeds the capillary pressure, pushing the merged droplet out of the chamber (Fig. 17.9). The process of droplet merging depends on the pillar geometry, interfacial tension, flowrate ratio and viscosity of the continuous and dispersed streams.

Active Merging
Active methods employ on-chip structures and control electronics to achieve droplet merging. It includes electrical, thermal and optical methods. Electrical-based methods include dielectrophoresis (DEP) [17.13] and electrowetting-on-dielectric (EWOD) [17.14] force fields where the actuation of electrodes induces the merging. Droplets are stacked up one by one over a series of electrodes and the controlled actuation of a pair of adjacent electrodes coalesce the packed droplets (Fig. 17.10). It is also possible to actuate the adjacent electrodes to move the droplets to the desired location and fuse them. Digital microfluidics is a field that controls droplet transport by the EWOD principle. Droplet merging can also be initiated by temperature. Temperature changes correlate to changes in the viscosity and drainage rate of the continuous phase resulting in droplet fusion [17.15]. Optical droplet merging techniques rely on the principle of optical tweezers but it is less attractive because of the lower throughput and lower actuation force [17.16].

Droplet Splitting
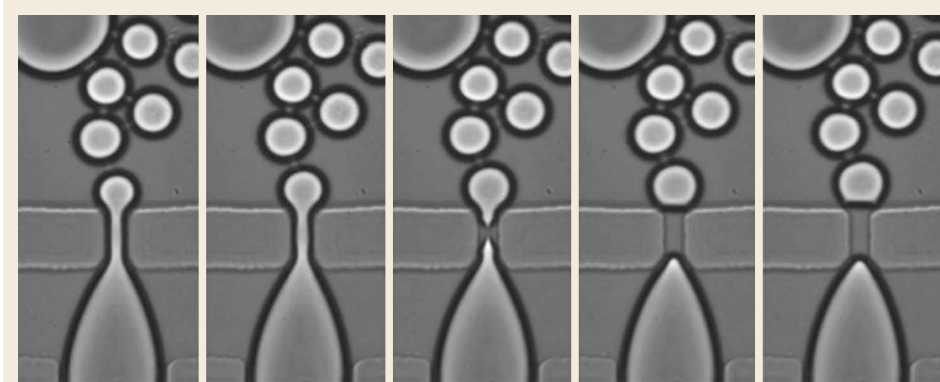Droplet splitting is a process of breaking the parent droplet into two daughter droplets. It is an important

Fig. 17.6a,b Droplet generation in flow-focusing geometry. Reprinted from [17.7] with the permission of AIP Publishing
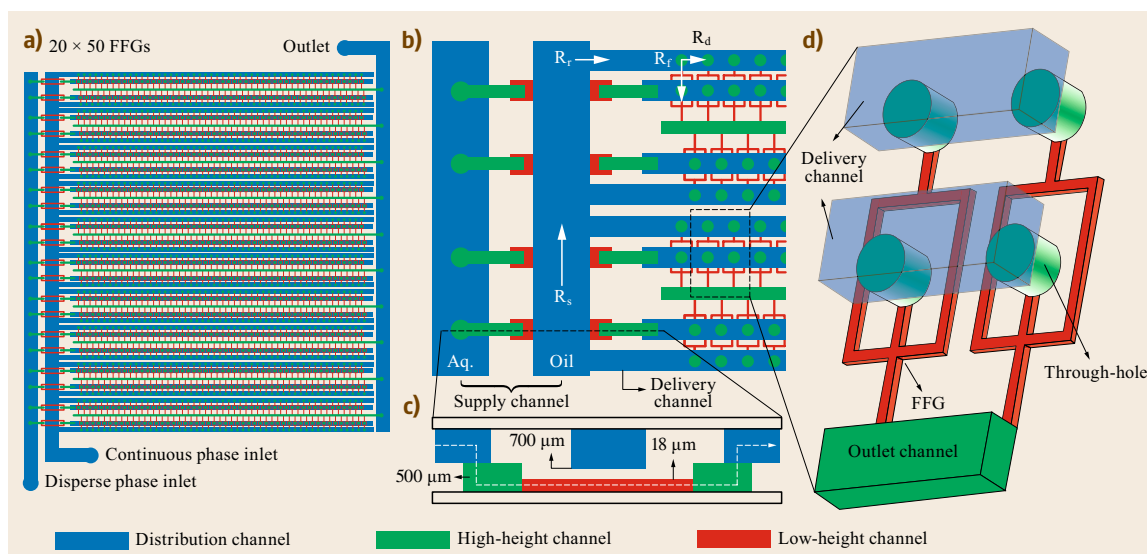
Fig. 17.7 Schematic of a 3D monolithic elastomer device (MED). **(a)** Design consists of 20 rows by 50 columns of flow focusing generators. **(b)** Ladder geometry and fluidic resistance modeling to ensure uniform distribution of solution in each flow focusing geometry. **(c)** Cross-sectional view of the device. **(d)** Fluid from the delivery channel enter the flow focusing geometry through the intermediate through-hole. Using this device, the droplet production rate can go up to 8.7 MHz
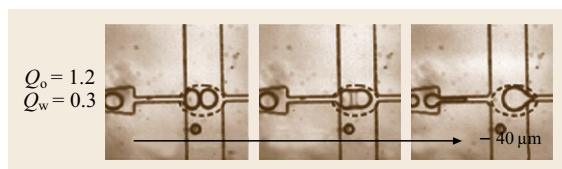

Fig. 17.8 Channel expansion design for droplet merging (after [17.11])

operation unit that increases throughput by parallelization. Droplet splitting is achieved using both passive and active methods. Passive techniques split the parent drop into two daughter droplets by shear force induced at the channel bifurcation point [17.11, 17, 18]. Given a constant flowrate, the size of the daughter droplet is determined by the hydraulic resistance of the channels (Fig. 17.11). Bifurcating channels with the same hydraulic resistances results in same shear forces on either half of the droplets, leading to symmetric splitting of the parent droplet (Fig. 17.12). Unequal channel resistances result in uneven droplet splitting such that the daughter droplet in the low-resistance channel is relatively larger than the one in the high resistance channel. Active splitting primarily uses electrical methods to perform droplet splitting. The EWOD technique can be used for active fission in digital microfluidics. The two electrodes on either end of the droplet are actuated while the center electrode is grounded. The electrodes on front and rear end of the droplet pulls the droplet in opposite directions in reference to the ground electrode, resulting in droplet splitting [17.19].

Assay Readout/Droplet Detection Technique

Sensing and detecting droplets is a critical operation unit in HTS of chemical or biological assays. It identifies the positive droplets from the population prior to droplet sorting for postprocessing. Light-induced fluorescent (LIF) detection via chemical labeling of biomolecules is a widely adopted detection technique [17.20]. In LIF, the excitation light source with a suitable wavelength is focused into the microfluidic chip. The excitation light can be either scattered or absorbed by particles, cells or biomolecules. If any of the molecules are stained by fluorophores, the resulting emission wavelength is captured by a detector, which can be a high-speed camera, confocal microscope, complementary metal-oxide-semiconductor (CMOS) sensors, or photomultiplier tubes (PMT). Recently, a combination of microlens array, reflective channel surface and high-speed camera was used for high-speed detection of droplets. This setup can screen droplets at a rate of 2 kHz per microlens [17.21]. Another detection technique relies on a CMOS sensor that can detect 40 pl droplets at 254 kHz [17.22] in the microfluidic chip. An integrated comprehensive droplet digital detection (IC3D) technique was reported in 2014, which can detect one positive droplet from 40 million droplets with 77% confidence [17.23]. Using
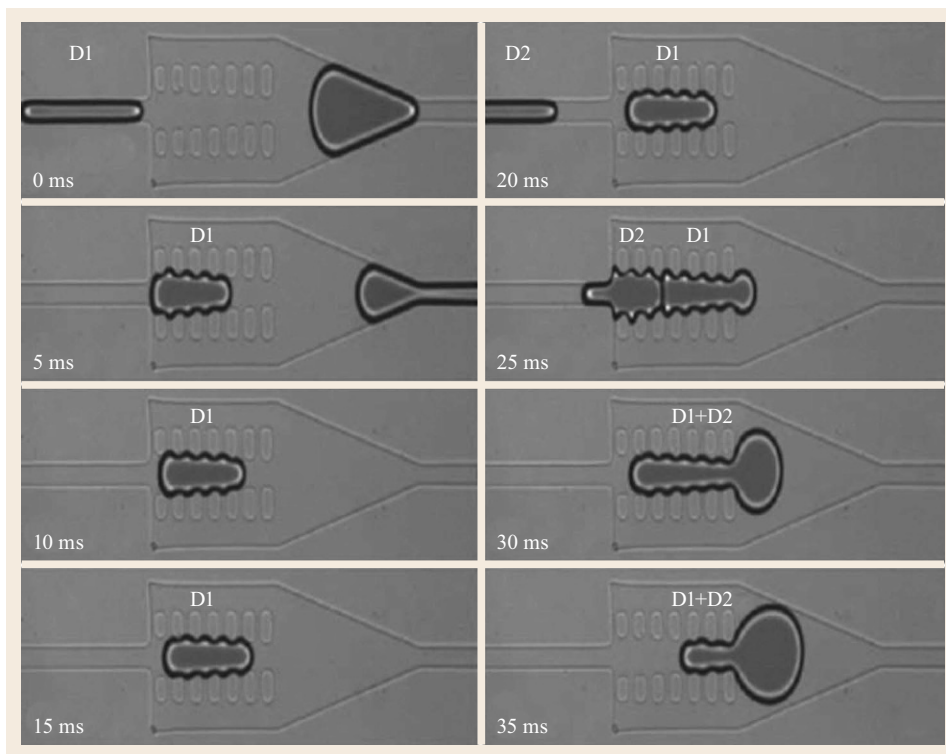
Fig. 17.9 Sequence of images illustrating the merging of two droplets induced by pillar structures. Reproduced from [17.12] with the permission of the Royal Society of Chemistry
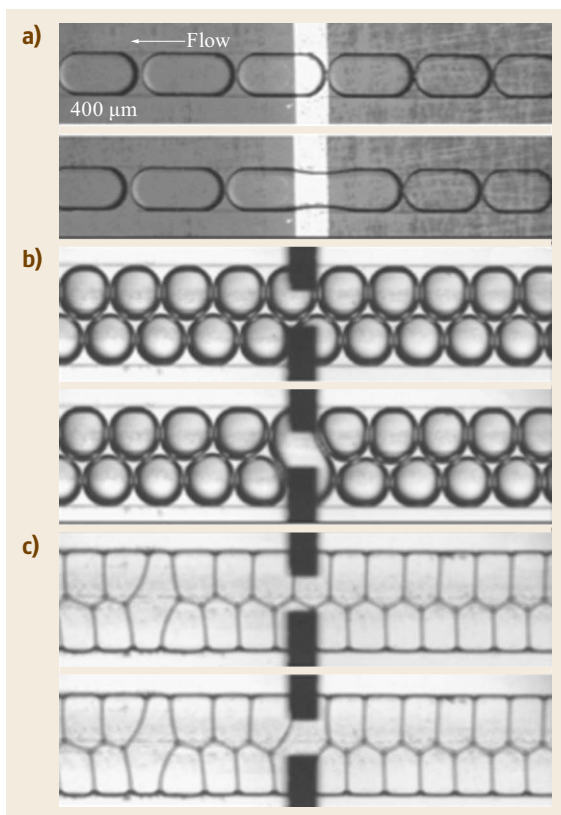

Fig. 17.10a−c Electro-coalescence of the droplets in a microchannel. When a low voltage pulse is applied, pairs of droplets coalesce at the gap between the electrodes. Coalescence of droplets within a **(a)** *bamboo* structure, **(b)** *zigzag* structure and **(c)** targeting of single lamellae in a foamlike zigzag structure. Reprinted from [17.14] with the permission of AIP Publishing ◀

this technique, the droplets collected in a glass cuvette are subjected to vertical and rotational translation and are detected by confocal microscopy (Fig. 17.13). In addition to LIF detection, there are other techniques such as electrochemical detection [17.24], mass spectroscopy [17.25], high-pressure liquid chromatography (HPLC) [17.26], surface enhanced Raman spectroscopy or the combinations of the above-mentioned methods [17.27].

Droplet Sorting

Droplet sorting enables the separation of individual droplets from a population as a function of its size or chemical payload. Droplet sorting can be grouped into two categories: passive and active.

Passive Sorting. As the name suggests, passive sorting techniques do not require any active components such as on-chip electrodes or additional instrumentation. Passive techniques are used to sort the droplets
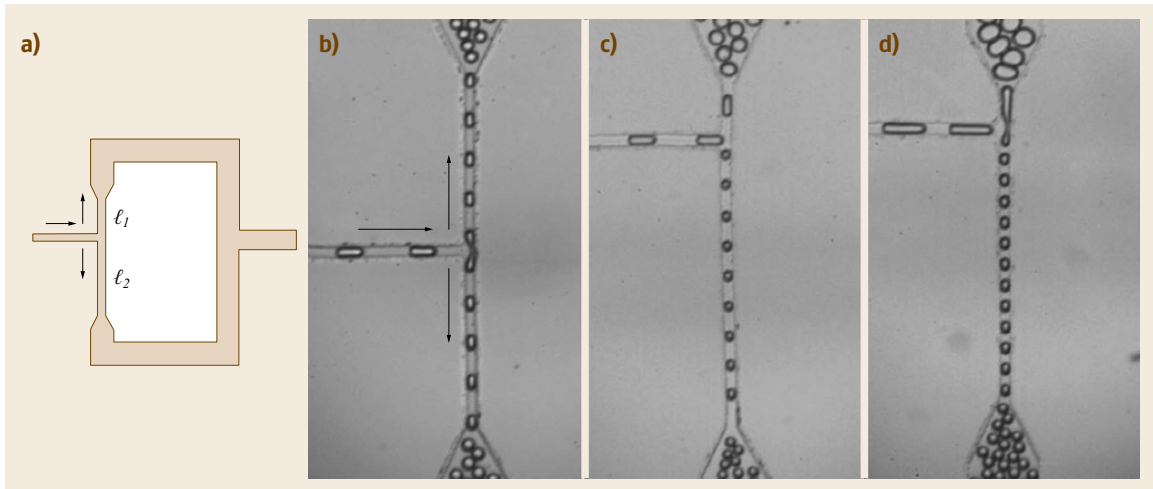
Fig. 17.11a–d Passive droplet splitting using a T-junction geometry. **(a)** Ratio of the two side arms of length ℓ_1 and ℓ_2 determines the size of daughter droplets. **(b)**, **(c)**, and **(d)**; the ratios of the arm lengths are 1:1, 1:5.2 and 1:8.1 respectively
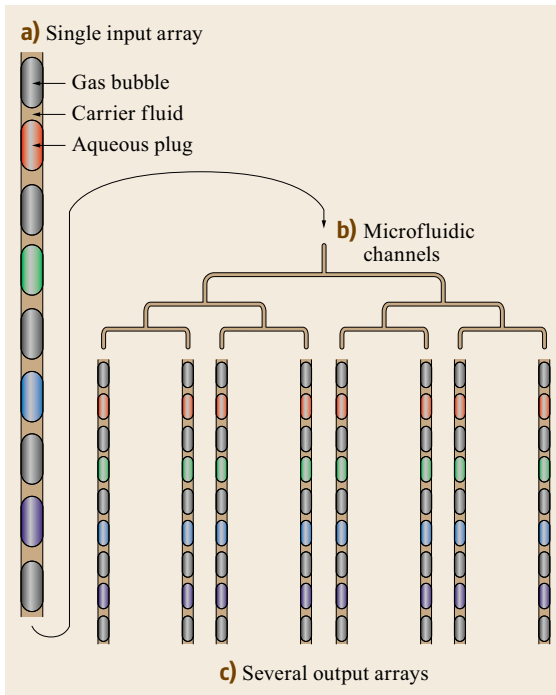
Fig. 17.12a–c Symmetric T-junction droplet splitter design for HTS (after [17.18])

based on their size. In 2007, *Tan* et al. demonstrated a hydrodynamic droplet sorting technique that utilized the channel geometry to alter the flow velocity that resulted in sorting [17.28]. Different sized droplets were successfully sorted into the respective outlets determined by the shear force ratio, which depends on the area of projection and shear rate imposed across the

droplet (Fig. 17.14). In 2008, *Chabert* et al. presented a hydrodynamic technique for cell encapsulation and subsequent sorting of the droplets at the channel bifurcation [17.29]. The cell-encapsulated droplets are larger than the empty droplets and thus gets sorted into the *left* outlet by the combined effect of lateral shear induced drift generated by the asymmetric oil flowrates and the steric interactions between the droplets at the bifurcation. In 2011, *Joensson* et al. demonstrated a deterministic lateral displacement (DLD) pillar array that could successfully sort 11 μm droplets from the 30 μm droplets at a frequency of 12 000 droplets/s [17.30]. In 2013, *Hatch* et al. reported a passive hydrodynamic droplet sorting technique by tuning the viscosity ratio (γ), which is defined as the ratio of the viscosity of the dispersed phase to the continuous phase [17.31]. If γ is between 0.5–10, the droplet migrates toward the region of high shear gradient (channel wall). For all other values of γ, the droplet migrates toward the low shear region (channel center).

Active Sorting. Active sorting techniques can sort droplets by their size and chemical contents, but require labeling and on-chip electrodes. In fluorescence-activated droplet sorting (FADS) [17.32] the fluorescent actuation of the on-chip electrodes redirects the droplets at the channel bifurcation via DEP forces [17.33]. This is an efficient technique capable of performing selective sorting of droplets based on their chemical contents (Fig. 17.15). Some of the other active techniques include piezoelectric actuated surface acoustic waves (SAW) [17.34], electrically actuated membrane valves [17.35], which hydrodynamically sort droplets, or laser-induced thermocapillary valves, which can
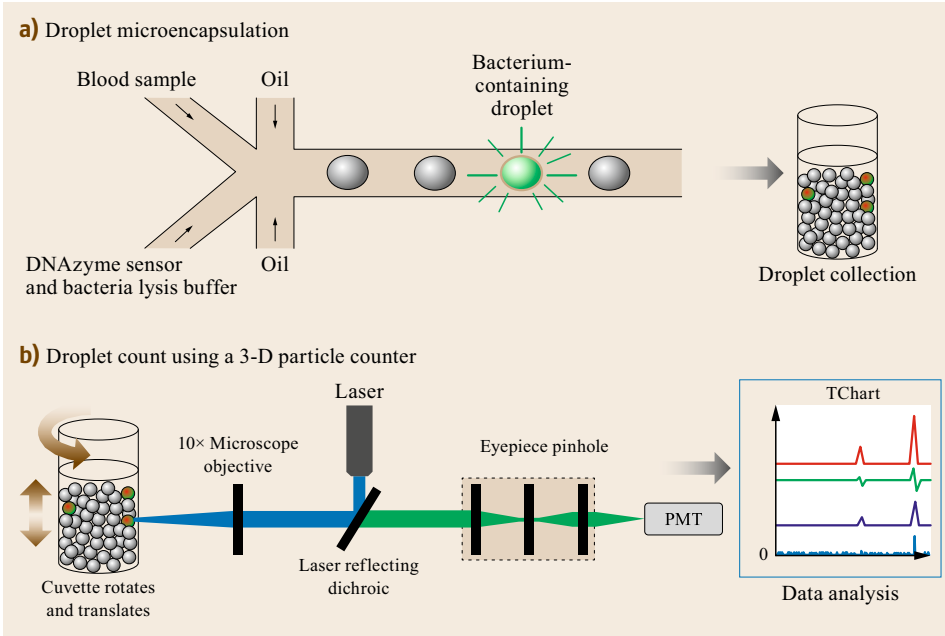
Fig. 17.13a,b Integrated Comprehensive Droplet Digital Detection (IC 3D) technique **(a)** Blood samples, DNAzyme sensors and bacteria lysis buffer is encapsulated in millions of droplets. DNAzyme sensor generates instantaneous signal in the droplets that contains bacterium. **(b)** Droplet are collected and analysed in a high-throughput 3D particle counter (after [17.23])
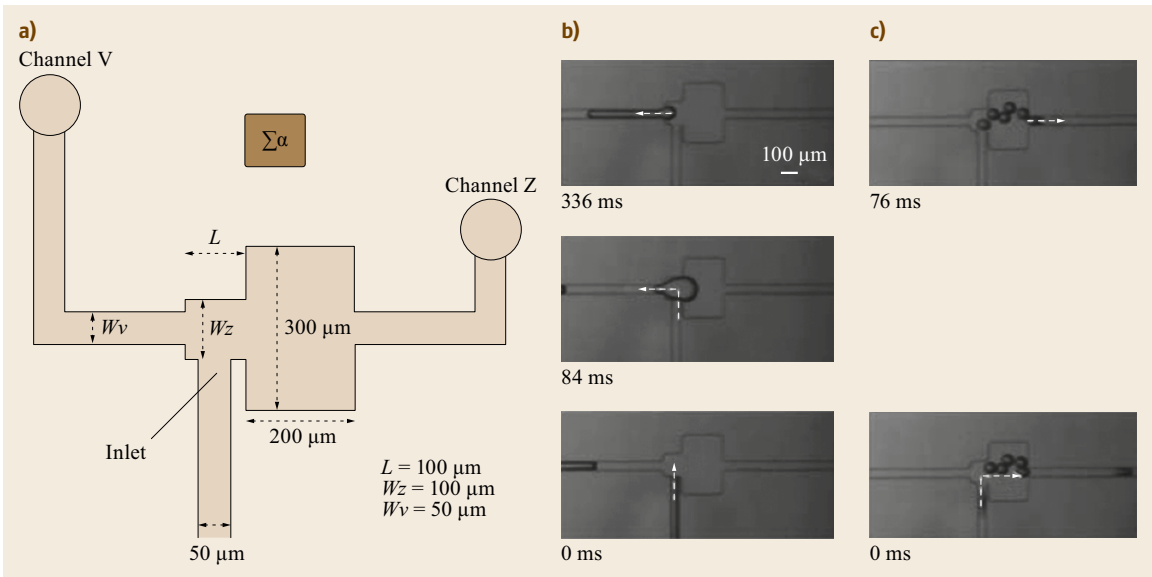
Fig. 17.14a–c Size based droplet sorting in a bifurcating microchannel **(a)** schematic of the device **(b)** large droplets are sorted into the channel V and **(c)** small droplets are sorted into channel Z. Sorting is based on the shear force ratio which depends on the area of projectionand shear rate imposed across the droplet (after [17.28])

block the advancement of droplets [17.36]. For a comprehensive understanding on various droplet unit operations, the reader is directed to an excellent review article [17.37].
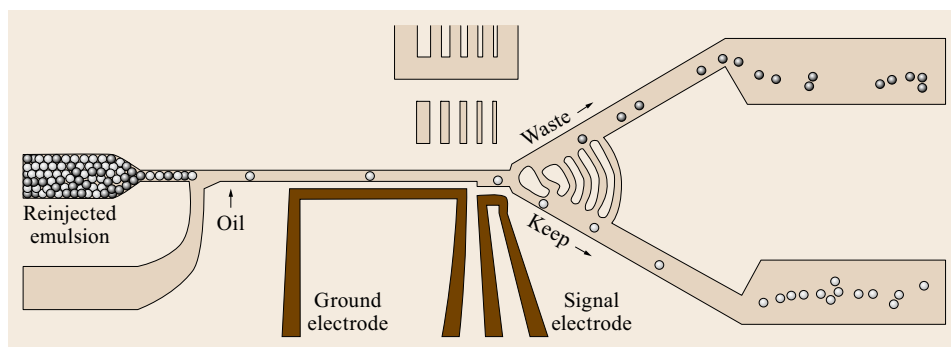
17.2 Overview of Current Trends in Droplet Microfluidic Technologies

The field of microfluidics originally emerged as an alternative to traditional, expensive, and bulky laboratory techniques. Costly reagents could be used in even smaller quantities, meaning that reaction time were shortened, translating to comparatively high resolution and sensitive detection. Microfluidic unit operations can emulate most basic laboratory operations, such as fluid dispensing, sample aliquot, sample mixing, and assay readout, at a fraction of the cost and time required with traditional methods. This enabled droplet microfluidic technology to rapidly emerge as a powerful platform to perform numerous applications in chemistry and biology. Academic interest in microfluidic technology first grew tremendously in the 1990s when the U.S. Department of Defense saw an opportunity for microfluidic systems to serve as portable detection units for biological and chemical threats, and in turn, developed a series of programs to stimulate microfluidic research in academic institutions.

The first microfluidic droplet generator was reported in 2001 by *Thorsen* et al. [17.5]. Since then, the technological developments in chemistry, biology and medicine have garnered substantial interest in applications enabled by droplet microfluidics. Further advancements in the microfabrication technologies using various substrate materials (e.g., glass, polymer) has led to the realization of many microfluidic droplet generator designs for control of droplet size, generation rate, and chemical composition [17.38]. The droplet based biomolecular assay was the first commercial success story of droplet technology. Bio-Rad Laboratories and Rain Dance Technologies successfully commercialized the droplet digital polymerase chain reaction (ddPCR) system in 2012 [17.39]. However, the droplet generation, thermocycling, and droplet readout are performed in three different instruments and the assay kit is still very expensive (> \$ 75 000). Several star-

tups including Intuitive Biosciences (Madison, WI) are working on ways to overcome the limitations and reduce costs. A droplet-based, fully integrated next-generation sequencing platform by GnuBIO Technologies is currently in the development stage [17.40]. The manufacturer claims that this instrument can perform scalable and accurate DNA sequencing that includes the additional steps of target enrichment and DNA amplification. If successful, this will be the first example of a commercial droplet-sequencing platform.

Another highly pursued and top-priority application in the field of droplet microfluidics is single-cell analysis [17.41]. Since the droplet microfluidic technology can easily generate cell-sized aqueous compartments, large populations of cells can be compartmentalized into independent monodisperse droplets. This enables the researchers to query the heterogeneity in cell populations at the single-cell level by performing sequencing or gene expression profiling in droplets, or to screen prospective drug variants against the target sample for cancer therapeutics [17.42, 43]. Droplet microfluidics has also emerged as a powerful tool for applications in directed evolution and synthetic biology. To engineer proteins and enzymes with novel activity, millions of genetic variants can be tested in individual microenvironments, evaluated, and isolated with high-throughput optical sorting methods [17.44].

Even with the tremendous progress of droplet microfluidics in recent years, there are still many technical challenges that researchers are working on to advance the field. One of the primary challenges pertains to high-throughput, sensitive detection and sorting of droplets. At present, there exists many efficient detection technologies, such as fluorescence detection, surface enhanced Raman spectroscopy, electrochemical detection, mass spectroscopy, HPLC and capillary elec-

trophoresis, but how well can these techniques work for high-throughput sensing and detection? Can we extract complete information from the picoliter volume reactors? As the miniaturization effort is still ongoing, droplet microfluidics will require further future dimensional scale-down in terms of the device size, droplet size and reagent volume, which would seriously challenge existing detection systems that have been designed for cell-sized structures.

Another area that requires improvement is the material used in the fabrication of microfluidic devices. In most research applications, polydimethylsiloxane (PDMS) is used to make the microfluidic chips. PDMS is transparent, flexible, biocompatible and permeable to gases; features that are suitable for culturing biomolecules and cells, but PDMS is also auto-fluorescent. If the signal-to-noise ratio is too low, fluorescent measurements can be compromised. PDMS also has low thermal conductivity, absorbs certain dyes, and swells in certain organic solvents (e.g., silicone oil). PDMS microfluidic devices are also typically polymerized in photolithographically patterned molds, which make them difficult to bulk manufacture and commercialize. An alternative to PDMS are injection-molded thermoplastic materials such as cyclic olefin copolymer (COC) chips. The comparatively low contact angle (82°) of COC, however, makes it difficult to generate water-in-oil droplets. The research is ongoing to improve the contact angle by appropriate surface treatments.

Another challenge for the future of droplet microfluidics is in the synthesis of ideal surfactants to perform assays within microfluidic channels. Although there are many commercially available organic solvents, proper incubation of the droplet emulsions requires standardized surfactants that limit the choice of organic solvents. A major problem encountered while incubating droplets is imperfect partitioning, leading to inter-droplet cross talk, which limits the stability of the emulsions, causing droplet shrinkage or coalescence. Since this is a relatively new and rapidly developing field, more work is ongoing to resolve these issues and challenges. As the field advances, one could foresee the development of integrated droplet microfluidic platforms that are portable, low-cost and autonomous. These platforms would be able to perform many complex biological processes in shorter times, yet with high efficiency and precision.

17.3 Fundamental Designs and Techniques for Microfluidic Generation of Droplets

Emulsions are liquid droplets suspended in another immiscible liquid. There are numerous ways to generate emulsions, such as atomization, chaotic mixing of two immiscible liquids, sprays and membrane emulsification. The consequence of this stochastic generation of emulsions leads to significant droplet size variation. Over the years, microfluidic technology emerged as a powerful tool to generate uniform droplet emulsions of femtoliter to nanoliter volumes at an ultrahigh throughput. As described earlier in the chapter, microfluidic droplet generators can be categorized into active and passive methods. Active droplet generators require additional instrumentation including on-chip devices and control electronics whereas passive methods rely on the interacting flow fields and interfacial instabilities to generate droplets. Passive droplet generation can be grouped into three categories:

1. Coflowing geometry
2. Cross-flowing or T-junction geometry
3. Flow-focusing geometry.

The schematic of all three geometries are shown in Fig. 17.16. In all three cases, the dispersed phase and the continuous phase are introduced separately into the microchannels by a pressure-driven flow that is driven either at constant volumetric flowrates (using syringe pumps) or constant pressures (by pressure regulator and solenoid valves). The two phases meet at a channel junction and eventually the dispersed phase pinches off by free surface instability. The droplet pinch-off process is a result of the competition between the local fluid stress (viscous force), which causes the interface to deform while the capillary pressure (interfacial tension force) resists the deformation. The ratio of viscous stress to the capillary stress is defined by a dimensionless number called the capillary number (Ca)

$$Ca = \mu_c \frac{V}{\sigma},$$

where μ_c is the viscosity of the continuous phase, V is the velocity of the continuous phase and σ is the interfacial tension between continuous phase and dispersed phase. Another two dimensionless parameters that directly influence droplet breakup are the volumetric flowrate ratio (φ)
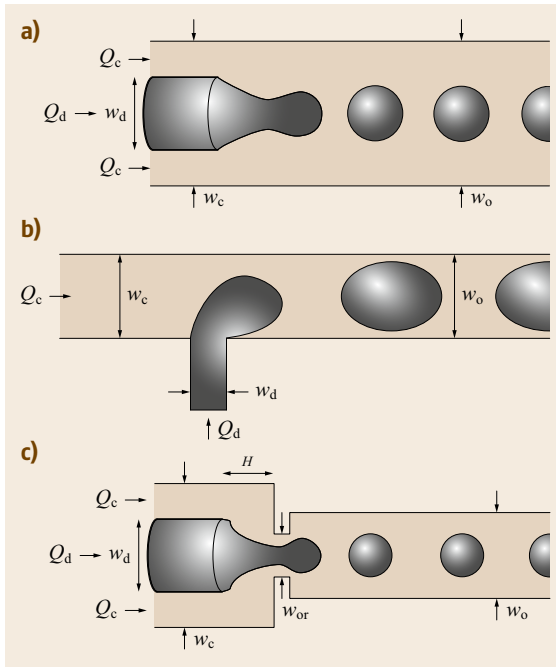
$$\varphi = \frac{Q_d}{Q_c},$$

Fig. 17.16a–c Schematic of three major passive droplet generation geometries **(a)** coflowing geometry **(b)** cross-flowing or T-junction geometry **(c)** flow-focusing geometry. (After [17.38])

where Q_d is the volumetric flowrate of the dispersed phase and Q_c is the volumetric flowrate of the continuous phase, and the viscosity ratio (γ)

$$\gamma = \frac{\mu_d}{\mu_c} ,$$

where μ_d and μ_c are the viscosity of the dispersed and continuous phases, respectively.

17.3.1 Passive Droplet Generation Techniques

Coflowing Geometry
This is the simplest geometry to generate uniform droplets. The geometry consists of a set of concentric channels, where the dispersed phase is introduced through the inner concentric channel while the continuous phase flows through the exterior [17.45]. The configuration is illustrated in Fig. 17.1a. Two droplet generation regimes are observed in this configuration, dripping and jetting. The transition from dripping to jetting is observed if the continuous phase increases above a critical velocity [17.46]. The critical velocity is a function of dispersed phase velocity, interfacial tension and viscosity ratio (γ). The critical velocity decreases

with increasing dispersed phase velocity and decreasing interfacial tension. Droplet size is a function of the volumetric flowrate (φ) and interfacial tension (σ). An increase in φ results in an increase in droplet size. Higher continuous flowrates exert more shear stress on the dispersed phase interface that result in smaller droplets. Similarly, an increase in σ makes the interface weaker and hence the dispersed phase can easily break off into smaller droplets. It is shown that the viscosity ratio (γ) has no significant effect on the droplet size over a wide range of continuous phase flowrates. In this regime, the predicted droplet size is given by the nondimensional equation [17.45]

$$d_1^3 - \left(1 + \frac{1}{3Ca}\right)d_1^2 - \frac{\varphi}{\alpha}d_1 + \frac{\varphi}{\alpha} = 0 ,$$

where d_1 is the ratio of droplet diameter (d) to the diameter of the inner capillary tube and $\alpha = A_d/A_c$ is the ratio of the two cross-sectional areas of the inner and outer capillary tube. If the dispersed phase flowrate is slow enough, the above equation simplifies to

$$d_1 \approx 1 + \frac{1}{3Ca} .$$

The droplet breakup and the size depends on the viscous stress and the capillary pressures. Using this geometry, highly monodisperse droplets with diameters in the range of few hundred micrometers are produced with polydispersity values ranging from 1 to 2%.

Notably, the wettability of the channel wall is crucial in determining which phase is dispersed. If the channel wall is hydrophobic (e.g., PDMS), the oil phase will wet the wall and form the continuous phase. In that case, the aqueous phase will form the droplets. Conversely, if the channel wall is hydrophilic (e.g., silicon), then the aqueous phase will form the continuous phase while the oil phase will form the droplets.

Cross–Flow or T–Junction Geometry
This is one of the simplest and common microfluidic geometries to generate monodisperse droplets [17.4, 47]. Depending on how the droplet phase fills the junction, the T-Junction geometry can be grouped into two categories, unconfined geometry and confined geometry.

Unconfined Geometry. In the unconfined geometry, the width of the continuous phase channel is at least five times larger than that of dispersed phase channel [17.48]. As the name suggests, the emerging droplets do not interact with the continuous phase channel walls and remain unconfined upon exiting the dispersed phase

inlet. The droplets generated from this geometry do not significantly disrupt the main channel flow, hence the droplet size is determined by the local shear stress at the junction. At a fixed dispersed phase flowrate, the size of the droplets decreases with increasing continuous phase flowrate. There are a few studies that show the droplet pinch-off occurring when the drag force exerted by the continuous phase flow overcomes the interfacial tension resisting the droplet deformation and the dispersed phase flowrate has little influence on the droplet breakup and the size [17.48, 49]. The droplet size in this geometry is given by

$$d_1^4 - 2d_1^3 + \frac{\epsilon}{2}d_1^2 + \frac{\alpha}{2C_\gamma Ca} = 0 ,$$

where $d_1 = d/D_c$ is the dimensionless number, which is the ratio of droplet diameter (d) to the hydraulic diameter (D_c) of the continuous phase channel

$$D_c = \frac{2w_c h}{w_c + h} ,$$

where w_c and h are the width of the continuous phase channel and height of the channel respectively

$$\alpha = \left(\frac{w_d}{D_c} \right)^2 ,$$

where w_d is the width of the dispersed phase channel,

$$C_\gamma = \frac{\left(3 + \frac{2}{\gamma} \right)}{\left(1 + \frac{1}{\gamma} \right)}$$

is the correction factor for viscosity ratio γ and ϵ is the ratio of droplet velocity to the average continuous flow velocity. The value ranges from $0 < \epsilon < 2$ and it depends on capillary number.

Confined Geometry. In the confined geometry, the width of the dispersed phase channel is comparable to that of the continuous phase [17.50]. The droplet phase completely obstructs the continuous phase channel (except for a thin Bretherton's film between the droplet and the wall), leading to an increase in the upstream pressure driving the breakup of the interface. Under these conditions, plugs are often generated instead of droplets. Plugs can be thought of an elongated droplet or the droplets with length in the flow direction greater than its width. The neck of the plug squeezes at a rate proportional to the average velocity of the continuous phase fluid and the plug fills at a rate proportional to the

dispersed phase flowrate [17.51, 52]. The final length of the plug is given by the expression

$$L_1 = \frac{L}{w_c} = 1 + \alpha\varphi ,$$

where α is the constant that depends on the width of the thinning neck. The equation shows that at low capillary number, the length of the plug depends only on the volumetric flowrate ratio. Above a critical capillary number, the viscosity ratio plays an important role in the droplet breakup, in contrast to the unconfined geometry. In the confined geometry, the droplet formation occurs within a specific range of flow conditions. If φ approaches unity, the dispersed-phase flowrate and the continuous-phase flowrate become equal, and it is observed that two phases flow parallel to each other without breakup.

Flow–Focusing Geometry. In this configuration the dispersed phase and the continuous phase are forced to pass through a small and narrow region in the microfluidic device [17.7]. The shear applied by the continuous phase over the dispersed phase results in droplet pinch-off. Three regimes are observed in this configuration:

1. Squeezing regime or geometrically controlled regime
2. Dripping regime
3. Jetting regime.

The transition between these regimes depends on the capillary numberand the flowrate ratio. In general, microfluidic droplet generation occurs at a capillary number within the range of $10^{-3}-10^1$. The squeezing regime occurs at low capillary numbers ($\approx 10^{-3}$). When the droplet phase enters the junction, it blocks the flow of the continuous phase and results in pressure buildup in the continuous phase inlets. The subsequent bidirectional shear results in the pressure buildup that pinches off the dispersed phase to form droplets. Notably, the pinch-off occurs right at the orifice. The droplet diameter in this regime is observed to be comparable to the orifice size and is larger than the other two regimes. As the capillary number increases, transition from squeezing regime to dripping regime is observed. In the dripping regime, the droplet breakup occurs within one characteristic diameter of the orifice [17.53, 54]. The interface after the breakup remains at a static location within the orifice. The droplets generated in this regime are smaller than the orifice diameter and are highly monodisperse (polydispersity $< 2\%$). At a fixed orifice size, the droplet diameter

decreases with increasing Ca and decreasing φ. The relationship between the droplet generation frequency (f), droplet spacing (s) and droplet velocity (U) is given by [17.55]

$$U = fs .$$

Zhou et al. [17.56] describe the droplet pinch-off mechanism in the dripping regime as a combination of a capillary instability, including Rayleigh capillary instability and end-pinching mechanism, shared with viscous drag exerted by the continuous phase on the droplet phase. The transition from the dripping to jetting regime occurs at a higher capillary number. In the jetting regime, as the name suggests, the dispersed phase protrudes like a long jet and it extends at least three orifice diameters outside the orifice exit. The droplets generated in this regime are polydisperse with a diameter larger than the dripping regime. The transition from the dripping to jetting regime occurs at a critical capillary number given by [17.54]

$$Ca_{cr} = \frac{t_{pinch}}{t_{growth}} = \frac{\mu_c Q_d}{\sigma R_{jet}^2} \approx 1 ,$$

when $Ca < Ca_{cr}$. The dripping regime is observed because of the interface instability, which will not allow the growth of a long jet, whereas for $Ca > Ca_{cr}$, the jetting regime is observed because the viscous stress will suppress the interface instability and allow the growth of a long jet. Droplet generation in coflowing, cross-flowing and flow-focusing geometries are illustrated in Fig. 17.17.

Passive droplet generators are widely used because of its ease of use and simplicity. Active droplets, though more complex, allow for better control over the droplet
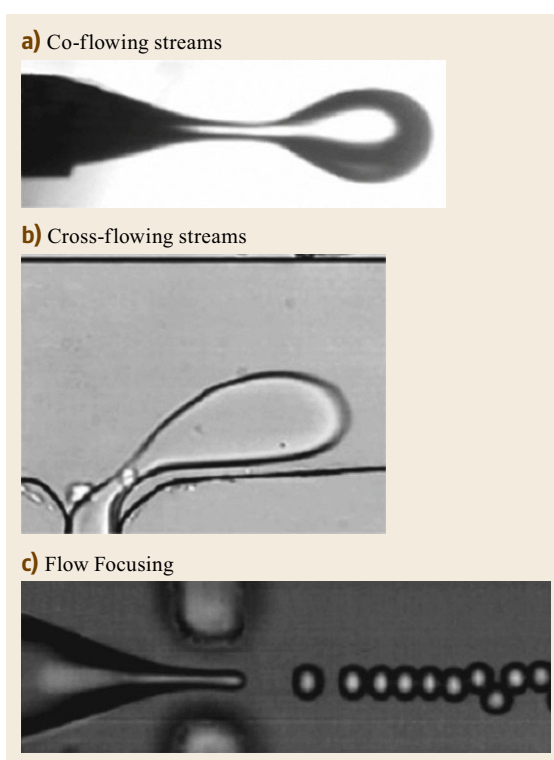

a) Co-flowing streams

b) Cross-flowing streams

c) Flow Focusing

Fig. 17.17a–c Droplet generation in all three geometries. **(a)** Coflowing geometry. **(b)** Cross-junction/T-junction geometry. **(c)** Flow-focusing geometry from [17.38], copyright IOP Publishing. Reproduced with permission all rights reserved

generation and production (ink jet printing technology). Active droplet generation employs piezoelectric transducers [17.57], membrane valves [17.58], electric fields [17.59] to initiate the droplet breakup.

17.4 Microfluidic Micro-/Nanodroplet Applications

Droplet microfluidics offers an excellent platform to conduct a diverse set of applications from chemical synthesis, particle manipulation, bioassays and drug discovery to point-of-care diagnostic chips [17.37, 60–62]. This section discusses the current and potential applications of droplet microfluidics.

17.4.1 Chemical Reactions in Droplets

Droplets act as isolated micro-/nanocontainers to perform chemical reactions. The exquisite control and manipulation of these droplet reactors enables one to conduct innumerable chemical reactions within the

droplets [17.4]. Droplet technology offers several advantages while performing the chemical reactions:

1. Reduced consumption of reagents
2. Less exposure to hazardous chemicals
3. Large surface-to-volume ratio enables better diffusion and mass flowrates
4. Recirculation within the droplets ensures proper mixing of the reactants
5. Scale up of the process by parallelization.

The hydrolysis reaction between *p*-nitro phenyl acetate and sodium hydroxide was performed in droplets.

Sodium hydroxide forms the droplet phase and the continuous phase contains *p*-nitro phenyl acetate. The reaction occurred as result of the mass transfer of *p*-nitro phenyl acetate into the droplet phase containing sodium hydroxide. Similar work has been reported to demonstrate the increased yield in droplet-based microreactor platforms [17.65]. The neutralization reaction can also be performed in droplets [17.66]. The acetic acid present in the continuous phase diffuse into the KOH/NaOH droplets and the color variation of the pH indicator is used to monitor the reaction and calculate the diffusion rates. It has been found that the diffusion rate is faster in small droplets than plugs. Other chemical reactions include precipitation reactions [17.67], anticoagulants [17.68], organic phase reactions [17.69] and the generation of cadmium selenide (CdSe) nanoparticles inside the droplets [17.63]. Separate droplets with different reagents were merged in a controlled environment to induce reactions inside the fused droplet to produce monodispersed nanoparticles (Fig. 17.18).
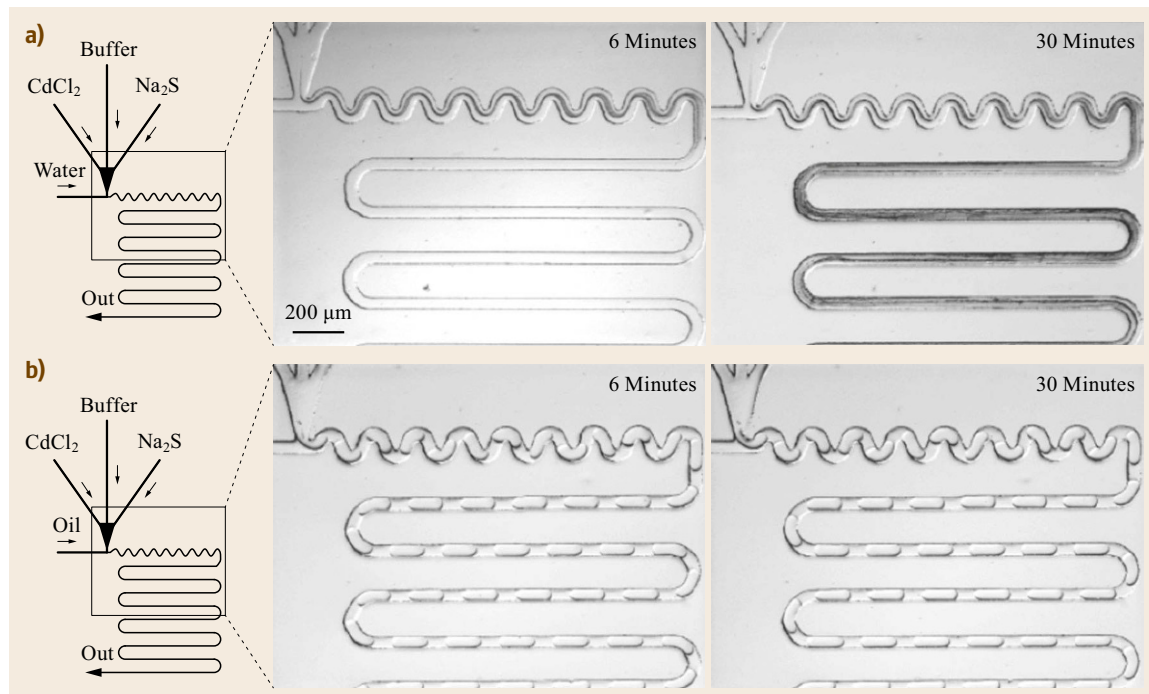

Fig. 17.18a,b Comparison of the nanoparticle (CdS) synthesis in (**a**) single-phase flow and (**b**) droplet phase. Unlike the droplet system, the single-phase system results in nanoparticle accumulation inside the channel and eventually leads to clogging. Reproduced from [17.63] with the permission of the Royal Society of Chemistry
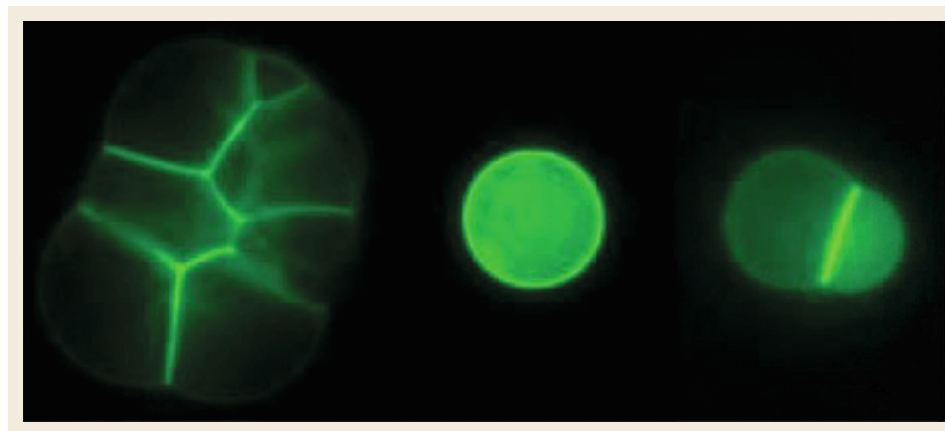

Fig. 17.19 A cell-like bioreactor produced by encapsulating the *E. coli* cell's free expression system in a phospholipid vesicle (after [17.64]), copyright 2004 National Academy of Sciences, USA

Part C | 17.4

17.4.2 Biomolecule Synthesis

Droplet microfluidics is an ideal platform to carry out controlled synthesis of a wide range of biomolecules including high- throughput directed evolution of proteins and polymerization chain reaction (PCR). The ability of droplet microfluidics to generate uniform and homogeneous droplets in a controlled environment is the fundamental requirement for the synthesis of artificial cells [17.71]. The formation of an artificial cell helps one study life's fundamental reactions. A cell-like bioreactor was produced by encapsulating the *E. coli* cell's free expression system in a phospho-

lipid vesicle [17.64]. The phospholipid bilayer acts as a semipermeable membrane that helps in the exchange of nutrients in and out of the cell (Fig. 17.19). *Huebner* et al. demonstrated protein expression by encapsulating single cells inside droplets and detecting the expression of fluorescent proteins within the cell [17.70]. This in-vitro protein expression in droplet vesicles offers potential applications in the high-throughput directed evolution of proteins (Fig. 17.20). In genomics, droplet microfluidics offer a compelling platform to perform PCR in droplets. Compared to the conventional approach, droplet-based PCR technology offers advantages in making the process quantitative and
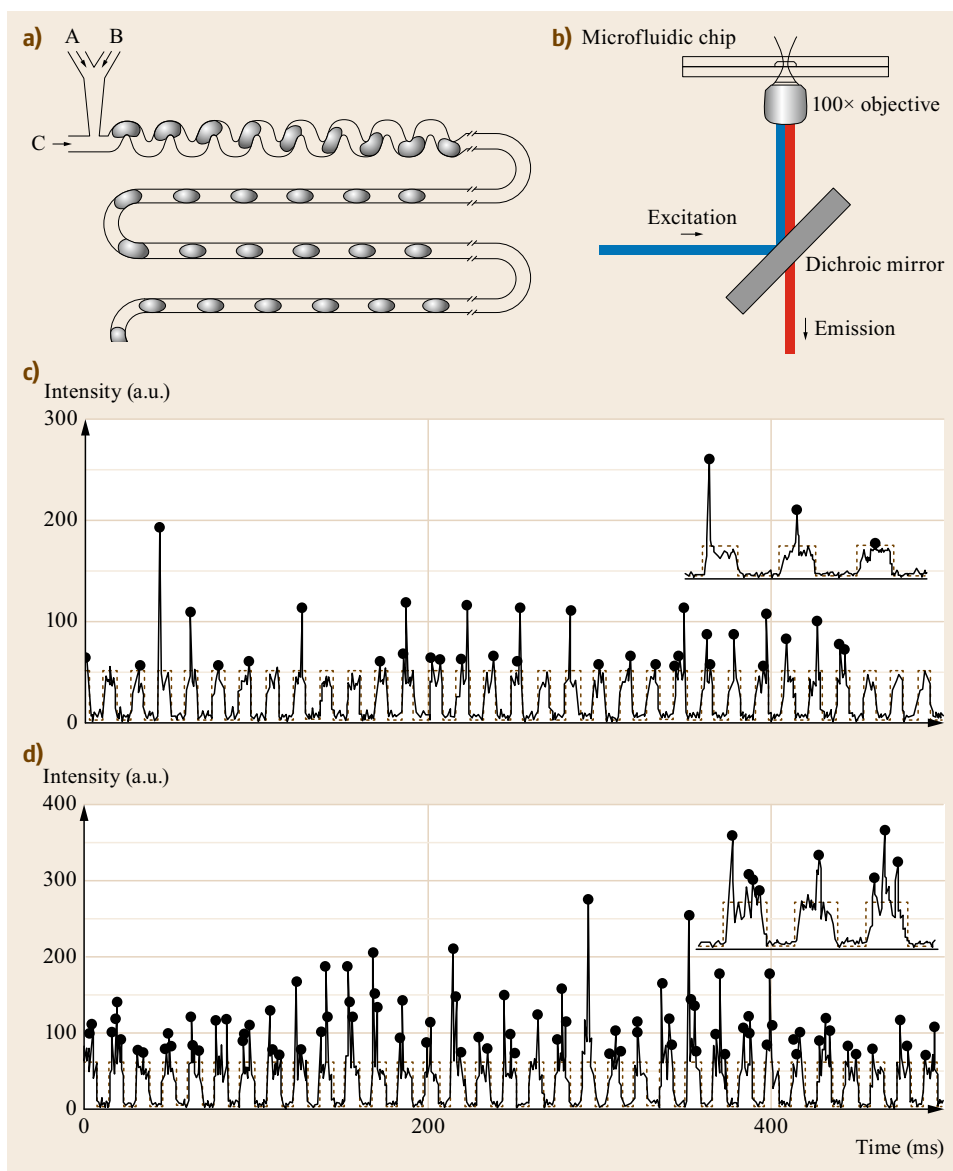
Fig. 17.20a–d Protein expression studies by encapsulating a single cell inside the droplet and detecting the expression of fluorescent proteins within the cell. Droplet-containing cells are distinguished by a vertical spike arising from the expressed fluorescent protein. Reproduced from [17.70] with the permission of the Royal Society of Chemistry

sensitive [17.72]. Droplet-based PCR also increases the amplification efficiency by minimizing the reagent dispersion and surface adsorption. Generally, droplet-based PCR is performed in two different ways. The first is a continuous flow-based approach. A droplet-based micro-oscillation flow PCR chip was designed and implemented by *Wang* et al. [17.73]. Injected droplets containing a PCR mixture, pass through the three distinct temperature zones (denaturation, extension and annealing) in the microfluidic channel to attain the required temperature transition. They successfully amplified human papillomavirus (HPV)-DNA samples and the PCR products were analyzed by gel electrophoresis. The group has also shown that the whole process takes less than 15 min, compared to 2 h for the conventional process. In the second method, microfluidic chips are used only for the generation and detection process [17.74]. This is the method that most commercial products utilize (Fig. 17.21). The process flow occurs in three steps:

1. Uniformly sized droplets with template DNA were created by a microfluidic drop generation device.
2. These droplets are transformed manually into 96-well plates and are placed in a thermocycling device that is programmed to control the temperature required for the DNA amplification.
3. Thermocycled droplets with amplicons are automatically transferred to the detection device, which has a microfluidic chip built into it.

The LIF detection system helps to quantitatively estimate the DNAexpression based on the fluorescence associated with each droplet.

17.4.3 Drug Discovery

In conjunction with high-speed and sensitive-detection technologies, such as LIF detection, mass spectroscopy, capillary electrophoresis, x-ray crystallography and HPLC, droplet microfluidics has the capability to perform HTS of target molecules against potential drugs. For example, to study the activity of a certain drug against the disease causing cells or proteins, both the labeled cells/proteins and drugs are encapsulated separately in the form of droplets using suitable droplet-generation configurations. These two specific droplet groups are subjected to droplet merging/fusion using appropriate passive or active fusion techniques. The product resulting from the reactions inside the fused droplet is picked up by fluorescence-detection techniques. Since the droplet generation frequency can reach 10 KHz, one can screen up to 10 000 droplets in one second, a speed that could revolutionize the high-throughput industry. As a result, the whole screen-
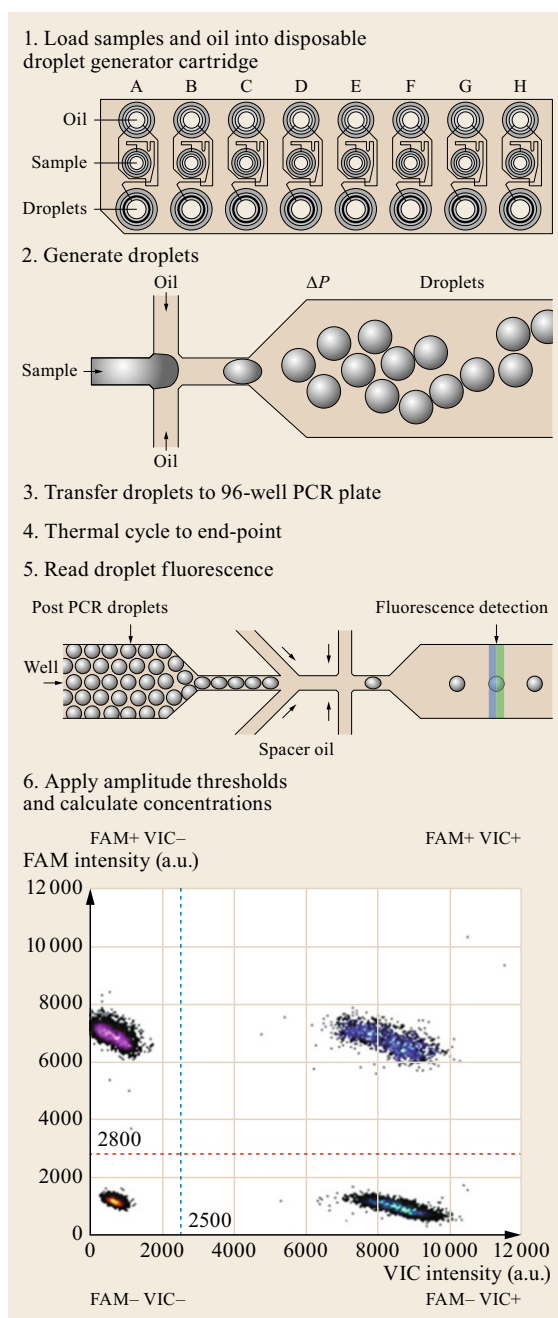

Fig. 17.21 BioRad's droplet PCR workflow

ing process has been transformed from conventional well plates to droplet technology. Another tool to perform high-throughput protein analysis is matrix-assisted desorption or ionization (MALDI). MALDI spectroscopy has been integrated with droplet technology to achieve high-throughput analysis of proteins and chemicals [17.75]. *Wheeler* et al. illustrated an EWOD-

based technique to purify the sample and analyze them using matrix-assisted laser desorption ionization-time of flight mass spectrometer (MALDI-TOF) mass spectroscopy [17.76]. In this platform, the whole process is automated but the common channels still allow for potential surface cross-contamination. Protein characterization can also be done by x-ray diffraction of protein crystals. Proteins (glucose isomerase, thaumatin and ferritin) are subjected to crystallization inside the droplets and were characterized using x-ray crystallography [17.77]. Another technique to characterize a drug compound is to perform kinetic studies to explore the activity of enzymes and chemicals. *Song* and *Ismagilov* have conducted kinetic measurements of ribonuclease A (RNase A) with millisecond temporal resolution [17.78]. The enzymatic activity was determined by the fluorescence resulting from the cleavage of a fluorogenic substrate by RNase A (Fig. 17.22). The intensity of the fluorescence is used to figure out the duration of the reaction process. In general, droplet microfluidics offers a standardized platform to perform

HTS of biomolecules. As such, the droplet microfluidics does not alter the format of the drug screening but it adds functionality and performance to the existing platform.

Directed evolution is another important application of droplet-based technology. Copies of genes or cells are distributed into each droplet compartment and are assayed for a specific phenotype. The positive droplets (the droplets containing the mutant genes) were sorted out and broken to recover the genotype for characterization [17.79]. Reverse-transcription PCR (RT-PCR) has emerged as a powerful technique to characterize the transcriptome of single cells in droplets [17.80]. This study will provide insights into the heterogeneity of the cells, their response to drugs or pathogens and the cause of various diseases. The single-cell transcriptomes are captured using the hydrogel microbeads, which are encapsulated in the droplets along with the cell. Entire transcriptomes of the cells were barcoded for identification purposes and this technique has reported a 13% mRNA capture efficiency (Fig. 17.23) [17.81].
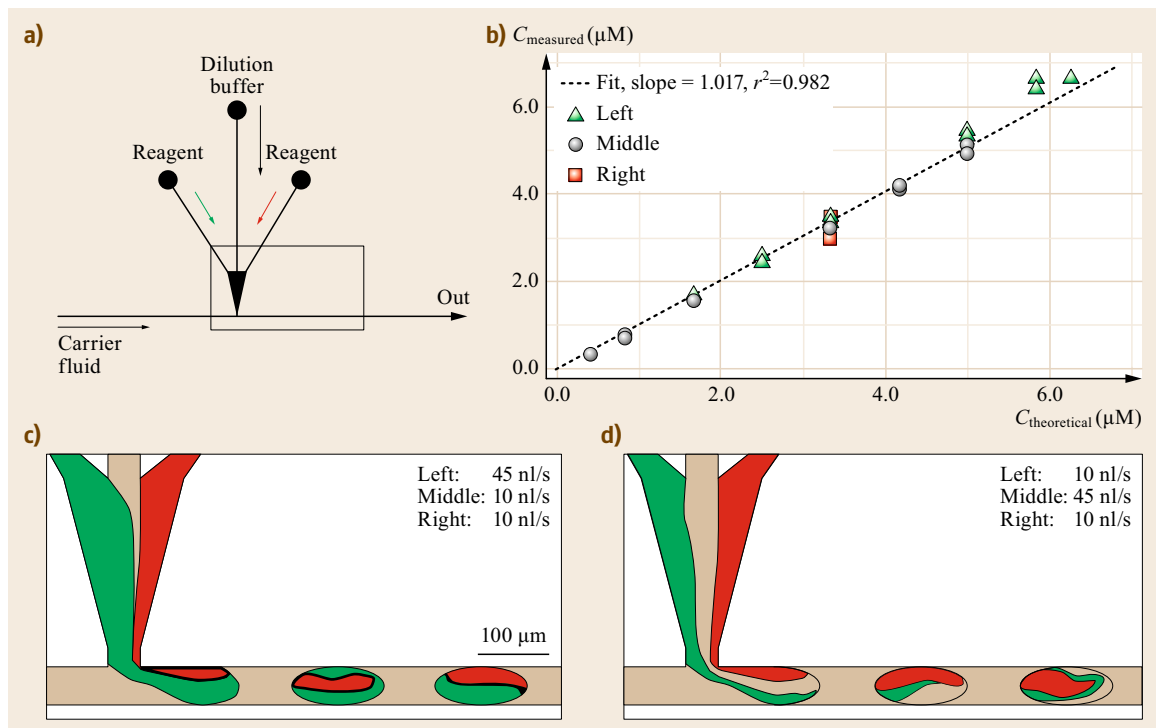

Fig. 17.22a−d Drug discovery in droplets. Demonstration of kinetic studies to explore the activity of enzymes and chemicals (after [17.78])
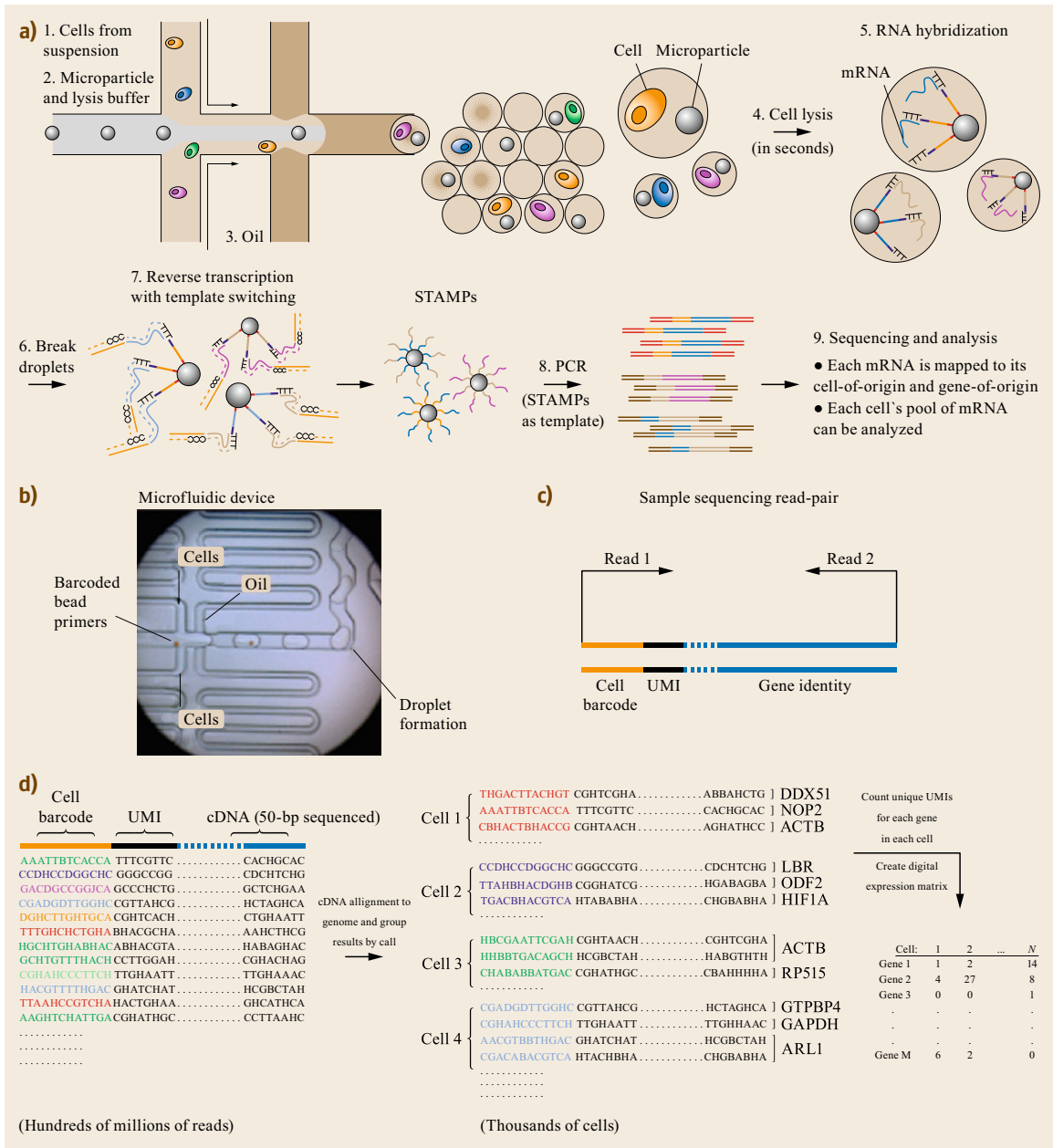
Fig. 17.23a–d The single-cell transcriptomes are captured using the hydrogel microbeads, which are encapsulated in the droplets along with the cell. Entire transcriptomes of the cells were barcoded for identification purposes and this technique has reported a 13% mRNA capture efficiency. Reprinted from [17.81] with permission from Elsevier

17.5 Conclusion

In this chapter, we introduced droplet microfluidic technology and its ability to manipulate fluids on the micro/nanoscale. The chapter also covered droplet generation techniques, current trends in droplet microfluidics and generic applications. The field of droplet microfluidics has matured over the last decade, as droplet microfluidic technologies are now being applied to a wide variety of commercial applications. There remain technical challenges to enable large networks of microfluidic operations in integrated devices that researchers are working on. However, the future of this promising technology is bright and it is predicted that droplet microfluidics will become an indispensable tool for a wide range of fluidic diagnostic platforms.

References

17.1   G.M. Whitesides: The origins and the future of microfluidics, Nature **442**(7101), 368–373 (2006)

17.2   T. Thorsen, S.J. Maerkl, S.R. Quake: Microfluidic large-scale integration, Science **298**(5593), 580–584 (2002)

17.3   J. Melin, S.R. Quake: Microfluidic large-scale integration: The evolution of design rules for biological automation, Annu. Rev. Biophys. Biomol. Struct. **36**(1), 213–231 (2007)

17.4   H. Song, D.L. Chen, R.F. Ismagilov: Reactions in droplets in microfluidic channels, Angew. Chem. Int. Ed. **45**(44), 7336–7356 (2006)

17.5   T. Thorsen, R.W. Roberts, F.H. Arnold, S.R. Quake: Dynamic pattern formation in a vesicle–generating microfluidic device, Phys. Rev. Lett. **86**(18), 4163–4166 (2001)

17.6   B. Zheng, J.D. Tice, R.F. Ismagilov: Formation of droplets of alternating composition in microfluidic channels and applications to indexing of concentrations in droplet–based assays, Anal. Chem. **76**(17), 4977–4982 (2004)

17.7   S.L. Anna, N. Bontoux, H.A. Stone: Formation of dispersions using flow focusing in microchannels, Appl. Phys. Lett. **82**(3), 364 (2003)

17.8   J. Shim, R.T. Ranasinghe, C.A. Smith, S.M. Ibrahim, F. Hollfelder, W.T.S. Huck, D. Klenerman, C. Abell: Ultrarapid generation of femtoliter microfluidic droplets for single–molecule–counting immunoassays, ACS Nano **7**(7), 5955–5964 (2013)

17.9   H.-H. Jeong, V.R. Yelleswarapu, S. Yadavali, D. Issadore, D. Lee: Kilo–scale droplet generation in three–dimensional monolithic elastomer device (3-D MED), Lab. Chip **15**(23), 4387–4392 (2015)

17.10   Y. Xia, G.M. Whitesides: Soft lithography, Annu. Rev. Mater. Sci. **28**(1), 153–184 (1998)

17.11   Y.-C. Tan, J.S. Fisher, A.I. Lee, V. Cristini, A.P. Lee: Design of microfluidic channel geometries for the control of droplet volume, chemical concentration, and sorting, Lab. Chip **4**(4), 292 (2004)

17.12   X. Niu, S. Gulati, J.B. Edel, A.J. deMello: Pillar–induced droplet merging in microfluidic circuits, Lab. Chip **8**(11), 1837 (2008)

17.13   P. Singh, N. Aubry: Transport and deformation of droplets in a microdevice using dielectrophoresis, Electrophoresis **28**(4), 644–657 (2007)

17.14   C. Priest, S. Herminghaus, R. Seemann: Controlled electrocoalescence in microfluidics: Targeting a single lamella, Appl. Phys. Lett. **89**(13), 134101 (2006)

17.15   J. Köhler, T. Henkel, A. Grodrian, T. Kirner, M. Roth, K. Martin, J. Metze: Digital reaction technology by micro segmented flow–components, concepts and applications, Chem. Eng. J. **101**(1–3), 201–216 (2004)

17.16   R.M. Lorenz, J.S. Edgar, G.D.M. Jeffries, D.T. Chiu: Microfluidic and optical systems for the on–demand generation and manipulation of single femtoliter–volume aqueous droplets, Anal. Chem. **78**(18), 6433–6439 (2006)

17.17   D. Link, S. Anna, D. Weitz, H. Stone: Geometrically mediated breakup of drops in microfluidic devices, Phys. Rev. Lett. (2004) doi:10.1103/PhysRevLett.92.054503

17.18   D.N. Adamson, D. Mustafi, J.X.J. Zhang, B. Zheng, R.F. Ismagilov: Production of arrays of chemically distinct nanolitre plugs via repeated splitting in microfluidic devices, Lab. Chip **6**(9), 1178 (2006)

17.19   S.K. Cho, H. Moon, C.-J. Kim: Creating, transporting, cutting, and merging liquid droplets by electrowetting–based actuation for digital microfluidic circuits, J. Microelectromech. Syst. **12**(1), 70–80 (2003)

17.20   J.J. Agresti, E. Antipov, A.R. Abate, K. Ahn, A.C. Rowat, J.-C. Baret, M. Marquez, A.M. Klibanov, A.D. Griffiths, D.A. Weitz: Ultrahigh–throughput screening in drop–based microfluidics for directed evolution, Proc. Natl. Acad. Sci. **107**(9), 4004–4009 (2010)

17.21   J. Lim, P. Gruner, M. Konrad, J.-C. Baret: Micro–optical lens array for fluorescence detection in droplet–based microfluidics, Lab. Chip **13**(8), 1472 (2013)

17.22   M. Kim, M. Pan, Y. Gai, S. Pang, C. Han, C. Yang, S.K.Y. Tang: Optofluidic ultrahigh–throughput detection of fluorescent drops, Lab. Chip **15**(6), 1417–1423 (2015)

17.23   D.-K. Kang, M.M. Ali, K. Zhang, S.S. Huang, E. Peterson, M.A. Digman, E. Gratton, W. Zhao: Rapid detection of single bacteria in unprocessed blood using integrated comprehensive droplet digital detection, Nat. Commun. **5**, 5427 (2014)

17.24   S. Liu, Y. Gu, R.B. Le Roux, S.M. Matthews, D. Bratton, K. Yunus, A.C. Fisher, W.T.S. Huck: The electrochemical detection of droplets in microfluidic devices, Lab. Chip **8**(11), 1937 (2008)

17.25 L.M. Fidalgo, G. Whyte, B.T. Ruotolo, J.L.P. Benesch, F. Stengel, C. Abell, C.V. Robinson, W.T.S. Huck: Coupling microdroplet microreactors with mass spectrometry: Reading the contents of single droplets online, Angew. Chem. Int. Ed. **48**(20), 3665–3668 (2009)

17.26 X.Z. Niu, B. Zhang, R.T. Marszalek, O. Ces, J.B. Edel, D.R. Klug, A.J. deMello: Droplet-based compartmentalization of chemically separated components in two-dimensional separations, Chem. Commun. (2009) doi:10.1039/b918100h

17.27 M.P. Cecchini, J. Hong, C. Lim, J. Choo, T. Albrecht, A.J. deMello, J.B. Edel: Ultrafast surface enhanced resonance raman scattering detection in droplet-based microfluidic systems, Anal. Chem. **83**(8), 3076–3081 (2011)

17.28 Y.-C. Tan, Y.L. Ho, A.P. Lee: Microfluidic sorting of droplets by size, Microfluid. Nanofluidics **4**(4), 343–348 (2007)

17.29 M. Chabert, J.-L. Viovy: Microfluidic high-throughput encapsulation and hydrodynamic self-sorting of single cells, Proc. Natl. Acad. Sci. **105**(9), 3191–3196 (2008)

17.30 H.N. Joensson, M. Uhlén, H.A. Svahn: Droplet size based separation by deterministic lateral displacement–separating droplets by cell-induced shrinking, Lab. Chip **11**(7), 1305 (2011)

17.31 A.C. Hatch, A. Patel, N.R. Beer, A.P. Lee: Passive droplet sorting using viscoelastic flow focusing, Lab. Chip **13**(7), 1308 (2013)

17.32 J.-C. Baret, O.J. Miller, V. Taly, M. Ryckelynck, A. El-Harrak, L. Frenz, C. Rick, M.L. Samuels, J.B. Hutchison, J.J. Agresti, D.R. Link, D.A. Weitz, A.D. Griffiths: Fluorescence-activated droplet sorting (FADS): Efficient microfluidic cell sorting based on enzymatic activity, Lab. Chip **9**(13), 1850 (2009)

17.33 K. Ahn, C. Kerbage, T.P. Hunt, R.M. Westervelt, D.R. Link, D.A. Weitz: Dielectrophoretic manipulation of drops for high-speed microfluidic sorting devices, Appl. Phys. Lett. **88**(2), 24104 (2006)

17.34 T. Franke, A.R. Abate, D.A. Weitz, A. Wixforth: Surface acoustic wave (SAW) directed droplet flow in microfluidics for PDMS devices, Lab. Chip **9**(18), 2625 (2009)

17.35 A.R. Abate, J.J. Agresti, D.A. Weitz: Microfluidic sorting with high-speed single-layer membrane valves, Appl. Phys. Lett. **96**(20), 203509 (2010)

17.36 C.N. Baroud, M.R. de Saint Vincent, J.-P. Delville: An optical toolbox for total control of droplet microfluidics, Lab. Chip **7**(8), 1029 (2007)

17.37 S.-Y. Teh, R. Lin, L.-H. Hung, A.P. Lee: Droplet microfluidics, Lab. Chip **8**(2), 198 (2008)

17.38 G.F. Christopher, S.L. Anna: Microfluidic methods for generating continuous droplet streams, J. Phys. Appl. Phys. **40**(19), R319–R336 (2007)

17.39 M. Baker: Digital PCR hits its stride, Nat. Methods **9**(6), 541–544 (2012)

17.40 A.R. Abate, T. Hung, R.A. Sperling, P. Mary, A. Rotem, J.J. Agresti, M.A. Weiner, D.A. Weitz: DNA sequence analysis with droplet-based microfluidics, Lab. Chip **13**(24), 4864 (2013)

17.41 S. Abalde-Cela, A. Gould, X. Liu, E. Kazamia, A.G. Smith, C. Abell: High-throughput detection of ethanol-producing cyanobacteria in a microdroplet platform, J. R. Soc. Interface **12**(106), 20150216–20150216 (2015)

17.42 P.S. Dittrich, A. Manz: Lab-on-a-chip: Microfluidics in drug discovery, Nat. Rev. Drug Discov. **5**(3), 210–218 (2006)

17.43 E. Brouzes, M. Medkova, N. Savenelli, D. Marran, M. Twardowski, J.B. Hutchison, J.M. Rothberg, D.R. Link, N. Perrimon, M.L. Samuels: Droplet microfluidic technology for single-cell high-throughput screening, Proc. Natl. Acad. Sci. **106**(34), 14195–14200 (2009)

17.44 A.C. Larsen, M.R. Dunn, A. Hatch, S.P. Sau, C. Youngbull, J.C. Chaput: A general strategy for expanding polymerase function by droplet microfluidics, Nat. Commun. **7**, 11235 (2016)

17.45 P.B. Umbanhowar, V. Prasad, D.A. Weitz: Monodisperse emulsion generation via drop break off in a coflowing stream, Langmuir **16**(2), 347–351 (2000)

17.46 C. Cramer, P. Fischer, E.J. Windhab: Drop formation in a co-flowing ambient fluid, Chem. Eng. Sci. **59**(15), 3045–3058 (2004)

17.47 G.F. Christopher, N.N. Noharuddin, J.A. Taylor, S.L. Anna: Experimental observations of the squeezing-to-dripping transition in T-shaped microfluidic junctions, Phys. Rev. E **78**(3), 36317 (2008)

17.48 J. Husny, J.J. Cooper-White: The effect of elasticity on drop creation in T-shaped microchannels, J. Non-Newton. Fluid Mech. **137**(1–3), 121–136 (2006)

17.49 J. Xu, G. Luo, G. Chen, J. Wang: Experimental and theoretical approaches on droplet formation from a micrometer screen hole, J. Membr. Sci. **266**(1–2), 121–131 (2005)

17.50 J.D. Tice, A.D. Lyon, R.F. Ismagilov: Effects of viscosity on droplet formation and mixing in microfluidic channels, Anal. Chim. Acta **507**(1), 73–77 (2004)

17.51 P. Garstecki, H. Stone, G. Whitesides: Mechanism for flow-rate controlled breakup in confined geometries: A route to monodisperse emulsions, Phys. Rev. Lett. (2005) doi:10.1103/PhysRevLett.94.164501

17.52 P. Garstecki, M.J. Fuerstman, H.A. Stone, G.M. Whitesides: Formation of droplets and bubbles in a microfluidic T-junction–scaling and mechanism of break-up, Lab. Chip **6**(3), 437 (2006)

17.53 S.L. Anna, H.C. Mayer: Microscale tipstreaming in a microfluidic flow focusing device, Phys. Fluids **18**(12), 121512 (2006)

17.54 A.S. Utada: Monodisperse double emulsions generated from a microcapillary device, Science **308**(5721), 537–541 (2005)

17.55 T. Ward, M. Faivre, M. Abkarian, H.A. Stone: Microfluidic flow focusing: Drop size and scaling in pressureversus flow-rate-driven pumping, Electrophoresis **26**(19), 3716–3724 (2005)

17.56 C. Zhou, P. Yue, J.J. Feng: Formation of simple and compound drops in microfluidic devices, Phys. Fluids **18**(9), 92105 (2006)

17.57 B. Beulen, J. de Jong, H. Reinten, M. van den Berg, H. Wijshoff, R. van Dongen: Flows on the nozzle

Part C | 17

plate of an inkjet printhead, Exp. Fluids **42**(2), 217–224 (2007)

17.58   H. Willaime, V. Barbier, L. Kloul, S. Maine, P. Tabeling: Arnold tongues in a microfluidic drop emitter, Phys. Rev. Lett. (2006) doi:10.1103/PhysRevLett.96.054501

17.59   O. Ozen, N. Aubry, D.T. Papageorgiou, P.G. Petropoulos: Monodisperse drop formation in square microchannels, Phys. Rev. Lett. (2006) doi:10.1103/PhysRevLett.96.144501

17.60   D.T. Chiu, R.M. Lorenz, G.D.M. Jeffries: Droplets for ultrasmall-volume analysis, Anal. Chem. **81**(13), 5111–5118 (2009) doi:10.1021/ac900306q

17.61   A. Huebner, S. Sharma, M. Srisa-Art, F. Hollfelder, J.B. Edel, A.J. deMello: Microdroplets: A sea of applications?, Lab. Chip **8**(8), 1244 (2008)

17.62   A.K. Price, B.M. Paegel: Discovery in droplets, Anal. Chem. **88**(1), 339–353 (2016)

17.63   I. Shestopalov, J.D. Tice, R.F. Ismagilov: Multi-step synthesis of nanoparticles performed on millisecond time scale in a microfluidic droplet-based system, Lab. Chip **4**(4), 316 (2004)

17.64   V. Noireaux, A. Libchaber: A vesicle bioreactor as a step toward an artificial cell assembly, Proc. Natl. Acad. Sci. **101**(51), 17669–17674 (2004)

17.65   B. Ahmed, D. Barrow, T. Wirth: Enhancement of reaction rates by segmented fluid flow in capillary scale reactors, Adv. Synth. Catal. **348**(9), 1043–1048 (2006)

17.66   J.R. Burns, C. Ramshaw: The intensification of rapid reactions in multiphase systems using slug flow in capillaries, Lab. Chip **1**(1), 10 (2001)

17.67   K.-I. Sotowa, K. Irie, T. Fukumori, K. Kusakabe, S. Sugiyama: Droplet formation by the collision of two aqueous solutions in a microchannel and application to particle synthesis, Chem. Eng. Technol. **30**(3), 383–388 (2007)

17.68   H. Song, H.-W. Li, M.S. Munson, T.G. Van Ha, R.F. Ismagilov: On-chip titration of an anticoagulant argatroban and determination of the clotting time within whole blood or plasma using a plug-based microfluidic system, Anal. Chem. **78**(14), 4839–4849 (2006)

17.69   Z.T. Cygan, J.T. Cabral, K.L. Beers, E.J. Amis: Microfluidic platform for the generation of organic-phase microreactors, Langmuir **21**(8), 3629–3634 (2005)

17.70   A. Huebner, M. Srisa-Art, D. Holt, C. Abell, F. Hollfelder, A.J. deMello, J.B. Edel: Quantitative detection of protein expression in single cells using droplet microfluidics, Chem. Commun. (2007) doi:10.1039/b618570c

17.71   M.S. Long, C.D. Jones, M.R. Helfrich, L.K. Mangeney-Slavin, C.D. Keating: Dynamic microcompartmentation in synthetic cells, Proc. Natl. Acad. Sci. **102**(17), 5920–5925 (2005)

17.72   V. Taly, D. Pekin, A.E. Abed, P. Laurent-Puig: Detecting biomarkers with microdroplet technology, Trends Mol. Med. **18**(7), 405–416 (2012)

17.73   W. Wang, Z.-X. Li, R. Luo, S.-H. Lü, A.-D. Xu, Y.-J. Yang: Droplet-based micro oscillating-flow PCR chip, J. Micromech. Microeng. **15**(8), 1369–1377 (2005)

17.74   B.J. Hindson, K.D. Ness, D.A. Masquelier, P. Belgrader, N.J. Heredia, A.J. Makarewicz, I.J. Bright, M.Y. Lucero, A.L. Hiddessen, T.C. Legler, T.K. Kitano, M.R. Hodel, J.F. Petersen, P.W. Wyatt, E.R. Steenblock, P.H. Shah, L.J. Bousse, C.B. Troup, J.C. Mellen, D.K. Wittmann, N.G. Erndt, T.H. Cauley, R.T. Koehler, A.P. So, S. Dube, K.A. Rose, L. Montesclaros, S. Wang, D.P. Stumbo, S.P. Hodges, S. Romine, F.P. Milanovich, H.E. White, J.F. Regan, G.A. Karlin-Neumann, C.M. Hindson, S. Saxonov, B.W. Colston: High-throughput droplet digital PCR system for absolute quantitation of DNA copy number, Anal. Chem. **83**(22), 8604–8610 (2011)

17.75   T. Hatakeyama, D.L. Chen, R.F. Ismagilov: Microgram-scale testing of reaction conditions in solution using nanoliter plugs in microfluidics with detection by MALDI-MS, J. Am. Chem. Soc. **128**(8), 2518–2519 (2006)

17.76   A.R. Wheeler, H. Moon, C.A. Bird, R.R.O. Loo, C.-J. Kim, J.A. Loo, R.L. Garrell: Digital microfluidics with in-line sample purification for proteomics analyses with MALDI-MS, Anal. Chem. **77**(2), 534–540 (2005)

17.77   B.T.C. Lau, C.A. Baitz, X.P. Dong, C.L. Hansen: A complete microfluidic screening platform for rational protein crystallization, J. Am. Chem. Soc. **129**(3), 454–455 (2007)

17.78   H. Song, R.F. Ismagilov: Millisecond kinetics on a microfluidic chip using nanoliters of reagents, J. Am. Chem. Soc. **125**(47), 14613–14619 (2003)

17.79   B. Kintses, C. Hein, M.F. Mohamed, M. Fischlechner, F. Courtois, C. Lainé, F. Hollfelder: Picoliter cell lysate assays in microfluidic droplet compartments for directed enzyme evolution, Chem. Biol. **19**(8), 1001–1009 (2012)

17.80   D.J. Eastburn, A. Sciambi, A.R. Abate: Ultrahigh-throughput mammalian single-cell reverse-transcriptase polymerase chain reaction in microfluidic drops, Anal. Chem. **85**(16), 8016–8021 (2013)

17.81   E.Z. Macosko, A. Basu, R. Satija, J. Nemesh, K. Shekhar, M. Goldman, I. Tirosh, A.R. Bialas, N. Kamitaki, E.M. Martersteck, J.J. Trombetta, D.A. Weitz, J.R. Sanes, A.K. Shalek, A. Regev, S.A. McCarroll: Highly parallel genome-wide expression profiling of individual cells using nanoliter droplets, Cell **161**(5), 1202–1214 (2015)